A NUMERICAL STUDY OF THE NATURAL CONVECTION FLOW IN AN ASYMMETRICALLY HEATED VERTICAL CHANNEL: EFFECT OF HEAT SOURCE POSITION

Hemmer C.*, Popa C., Beaumont F. and Polidori G.
*Author for correspondence
GRESPI EA4694
University of Reims Champagne Ardenne,
Moulin de la Housse, BP 1039,
51687 Reims cedex 2, France,
E-mail: hemmerc@campa.fr

ABSTRACT

This paper deals with a numerical study of the natural convection flow in an asymmetrically heated vertical plane channel at Ra*=4.5.10^6. The objective of this study is then to highlight the influence of the heat source position at the heated wall on the behavior of both the return flow and the surface heat transfer. In order to neglect radiation, only the convective aspects related to natural convection are studied by carrying out simulations in water. Numerical simulations were performed for two-dimensional, laminar and unsteady flow using the finite volume approach. Based on the study of several heating distributions at wall, the influence of the incident thermal source location and of the dissipated power on the downward return flow is highlighted and on the heat transfer at wall as well.

INTRODUCTION

The heated vertical channel is representative of several problems such as the double-skin facade or Trombe wall, the chimney and the solar panel. Indeed, several studies [1], [2] have shown that the implementation of the concept of double-skin facade in a building with low inertia seems essential to improve the thermal comfort. Despite a great number of experimental and numerical studies concerning convective heat transfer in vertical channel heated or cooled, there is still a lack of fundamental knowledge in the main dynamic and thermal behaviours of such double skin facades in order to maximize their efficiency and minimize resulting energy losses. Numerical simulations of natural convection in agreement with experimental results can allow understanding complex phenomena involved in these cases. Although many experimental studies on the vertical channel have been conducted [3-5], the majority of studies have been limited to thermal measurements and studies concerning the flow dynamics are not so numerous in the literature [6-8]. Common to all these studies is the observation of an upward flow along the heated wall and a downward one along the opposed adiabatic wall which is Ra* dependent. For example, Elenbaas [3] has determined, in a vertical channel, several kinds of dynamical flow behaviours depending on the modified Rayleigh number (Ra*), which is based on the channel width (b) and the ratio (A/b) where A is the heated length at wall.

NOMENCLATURE

A	[m]	Heated length
b	[m]	Channel wall spacing
C_p	[J/kg.K]	Specific heat capacity
g	[m/s^3]	Acceleration of gravity
H	[m]	Height of the heating zone
k	[W/m.K]	Thermal conductivity
L	[m]	Separation length
l	[m]	Characteristic length
$\overline{Nu}$	[-]	averaged Nusselt number
P	[W]	Dissipated power
P*	[Pa]	Driving pressure
Pr	[-]	Prandtl number
Ra	[-]	Rayleigh number
Ra*	[-]	Modified Rayleigh number
R_f	[-]	Aspect ratio
T	[K]	Temperature
u	[m/s]	Velocity component
v	[m/s]	Velocity component
x	[m]	Cartesian axis direction
y	[m]	Cartesian axis direction

Special characters

β	[1/K]	Volume expansion coefficient
ϕ	[W/m^2]	Heat flux density
Φ	[W]	Heat flux
ρ	[kg/m^3]	Density
ν	[m^2/s]	Kinematic viscosity
μ	[Pa.s]	Dynamic viscosity

Subscripts

+	Adimensioned

These authors highlighted that for a low modified Rayleigh number (Ra*<100), the flow regime is fully developed over the entire width of the channel whereas for a high-modified Rayleigh number (Ra*>1000), the flow regime is of boundary layer-type along the heated wall with the presence of a reverse flow observed near the unheated wall. This flow structure was also observed by Manca et al. [9].

For such free convection coupled problem the knowledge of quantitative dynamic quantities is essential for the implement of numerical simulation codes. It is the reason why, in literature, numerical studies [10, 11, 12] have tempted to correlate the

geometrical and heating channel conditions with the dynamics and structure of the flow. Christian et al. [13] performed a numerical study of the natural convection flow in a ventilated façade, which was modelled by a vertical channel heated with a constant imposed temperature. The author showed for Ra* > 100 that convection is the principal mode of heat transfer. Corresponding correlations for the average Nusselt number were highlighted. Dehghan et al. [14] have studied natural convection in a vertical slot with two heat source elements.

The influence of both the heat generation rate and the separation distance between the sources has been investigated. It has been shown that wall conduction was important, and for substrates with a finite thermal conductivity, it is essential that the conjugate analysis be employed. The authors showed that the thermal interference between the heat sources was reduced increasing Ra*. In this study it was also observed that increasing the spacing between the sources had the effect to increase velocities within the channel. This led to an enhancement in the convective cooling of the upper located electronic component. A higher cold mass flow rate entering the cavity was observed when the spacing between the sources increased, which resulted in an increase in the convection heat transfer from both components. Fossa et al. [15] and Menezo et al. [16] studied the case of a non-uniformly heated channel at large numbers of modified Rayleigh channel. They studied a channel with an alternating periodic heating either on both sides or on a single. They measured the wall temperatures to determine the heat transfer in each zone. The authors underlined a new geometrical parameter in the non-uniform heating case. This geometrical parameter has been defined as the distance between the inlet channel and the beginning of the heating zone. They showed that an alternation between heated and unheated zones could enhance the heat transfer up to 20%, compared to a configuration of uniform heating at one wall. Desrayaud et al. [17] have interested the natural convection airflow in a vertical channel heated by a constant heat flux density on the half of one wall. This numerical study was carried out to investigate the sensitivity and the influence of several boundary conditions on the heat transfer in the channel. The authors have shown that when the fluid domain is limited only to the channel geometry, the pressure conditions at the inlet and the outlet of the channel are difficult to formulate. This non-exhaustive state of the art shows how this problem still questions.

The aim of this study is to analyse the configuration of heat source distribution in order to enhance the heat transfer by increasing the mass flow rate through the channel and consequently by decreasing the maximum temperature in the channel outlet. The investigations focus specifically on the influence of heat source distribution at the heated wall on the flow structure and heat transfer as well. Numerical transient results are presented after 30 minutes of heating which is a sufficient time to reach the establishment of a steady-state flow for such a configuration [10].

GEOMETRY SETUP

From a numerical point of view, two main approaches can be proposed to solve the problem of natural convection flow in the channel: either a complete simulation of the canal and its external environment, or a truncated simulation considering the single channel limited to its geometric limitations. The second approach is problematic (Desrayaud et al. [17]) in that boundary conditions at low and high channel interfaces are a priori unknown since the driving flow is located within the computation domain (Garnier [18]). It is the reason why the first approach has been here considered where interactions between the channel and its external environment are calculated. In the present numerical study, the same channel/environment geometry as used in the experimental work by Ospir et al. [10] and Polidori et al. [19] was considered. The channel is made up of two parallel planar vertical walls separated by a distance (b = 36 mm; $R_f = 5.2$). The reference case (called case 1) considered here is that of one wall composed of a heated central part (height A = 188 mm) and two unheated extensions (length A/2) respectively located at the bottom and top open ends of the channel while opposite wall remains entirely unheated throughout the duration of the simulations (Fig. 1).

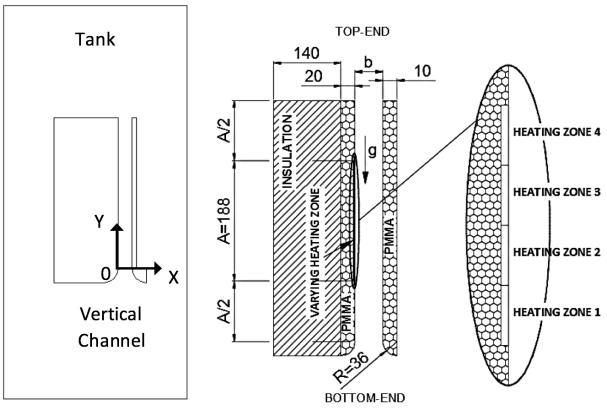

Figure 1 Geometry setup

In addition, for a better control of the flow conditions at the entrance, a quarter circle (R = 36mm) was added at the bottom of each wall. The channel is immerged in a vertical tank (500 x 500 x 1000 mm^3) made up of 20 mm thick Plexiglas® plates and filled with water which allows us to overcome the pressure boundary conditions at inlet and outlet of the channel (Desrayaud et al. [17]). The choice of water as working fluid leads to a negligible effect of heat transfer by radiation. Moreover, in this numerical study the conduction in the heating wall is not taken into account since Ospir et al. [10] observed experimentally no influence of the axial conduction for the same channel/environment geometry.

To study the influence of the heating distribution a variable heating area is considered and situated in the central part of channel; this zone of length A has been divided into four identical zones of high A/4. Case 1, which presents a uniform and continuous power distribution ($\phi = 510\ W/m^2$) on the A heating area, will be the reference case for this study. Cases 2, 3 and 4 present a uniform and continuous heating ($\phi = 1020\ W/m^2$) on the half of the heated area (A/2). The difference between these cases is the position of the heating zone: bottom (case 2), top (case 3) and middle (case 4). Case 5 corresponds to a discontinuous distribution of power ($\phi = 1020\ W/m^2$) to the heating area. It is recalled that dividing by

2 the heating length (case 2, 3, 4, 5) relative to the reference case (case 1), leads to double the heat flux density to keep the same thermal power.

PHYSICAL SETUP

The physical model of natural convection flow includes the transport equations of mass, momentum and energy. In this study the flow is considered as laminar, unsteady and two-dimensional. The fluid is Newtonian, incompressible and the physical properties (ρ, Cp, k, μ) of the fluid are temperature dependent [20-21] because Boussinesq assumption is not valid in the water, for temperature variations higher than 3 K. The channel is initially immersed in a tank filled with water at T = 289K.

The governing equations are: continuity equation, momentum equations and energy equation:

$$\frac{\partial u}{\partial x}+\frac{\partial v}{\partial y}=0 \quad (1)$$

$$\left(\frac{\partial u}{\partial t}+u\rho\frac{\partial u}{\partial x}+v\rho\frac{\partial u}{\partial y}\right)=-\frac{\partial P}{\partial x}+\frac{\partial}{\partial x}\left(\mu\frac{\partial u}{\partial x}\right)+\frac{\partial}{\partial y}\left(\mu\frac{\partial u}{\partial y}\right)+\frac{\partial u}{\partial x}\frac{\partial \mu}{\partial x}+\frac{\partial v}{\partial x}\frac{\partial \mu}{\partial y}-\rho g_x \quad (2)$$

$$\left(\frac{\partial v}{\partial t}+u\rho\frac{\partial v}{\partial x}+v\rho\frac{\partial v}{\partial y}\right)=-\frac{\partial P}{\partial y}+\frac{\partial}{\partial x}\left(\mu\frac{\partial v}{\partial x}\right)+\frac{\partial}{\partial y}\left(\mu\frac{\partial v}{\partial y}\right)+\frac{\partial u}{\partial y}\frac{\partial \mu}{\partial x}+\frac{\partial v}{\partial y}\frac{\partial \mu}{\partial y}-\rho g_y \quad (3)$$

$$\rho C_p\left(\frac{\partial T}{\partial t}+u\frac{\partial T}{\partial x}+v\frac{\partial T}{\partial y}\right)=\frac{\partial}{\partial x}\left(k\frac{\partial T}{\partial x}\right)+\frac{\partial}{\partial y}\left(k\frac{\partial T}{\partial y}\right) \quad (4)$$

To describe and compare the flow characteristics, dimensionless numbers have been introduced: aspect ratio (R_f), Prandtl number (Pr), Rayleigh number (Ra) and modified Rayleigh number (Ra^*) defined as:

$$R_f=\frac{A}{b};\ Pr=\frac{\nu}{a};\ Ra=\frac{g\beta\phi b^4}{k\nu^2}Pr;\ Ra^*=\frac{Ra}{R_f}=\frac{g\beta\phi b^4}{k\nu^2}\frac{b}{A}Pr \quad (5)$$

NUMERICAL METHOD

Transport equations of mass, momentum and energy (1) – (4) are solved numerically using the finite volume method [22]. This method is based on the spatial integration of transport equations relative to control volumes. The coupling between velocity and pressure is achieved with the algorithm Coupled algorithm that solves the equations of continuity and momentum simultaneously and gives an advantage to treat flows with a strong interdependence between dynamic and thermal fields. 2D numerical simulations are performed with ANSYS Fluent® CFD commercial software. A mesh independence study has been performed to ensure that the solution is independent on the grid size relative to the axial velocity profiles at the inlet and outlet of the channel. For example, in this study several mesh sizes inside the channel were tested (2100, 8400 and 36600 cells). The optimal mesh between the computation time (CPU) and accuracy is then the mesh with 8400 cells inside the channel which has 22000 cells in the whole calculation domain (Figure 2). During the transient computation, the optimal time step determined with respect to the flow velocity and the mesh size is 0.01s while the total CPU time is 92h for each case. The mesh of the fluid domain is, on the one hand, structured inside the channel (Δx = 0.4mm; Δy = 4mm) and on the other hand, unstructured and progressive outward from the tank. In this numerical study the Central-Differenced Scheme was used for the spatial discretization for diffusive term, the Second-Order Upwind Scheme for the convective term, the Second-Order Implicit formulation for the transient term and the Body Force Weighted Scheme for the continuity equation. The convergence criteria were based on the residuals resulting from the integration of the conservation equations over finite control volumes. During the iterative calculation process, these residuals were constantly monitored and carefully scrutinized. For all simulations performed in this study, converged solutions were achieved with residuals as low as 10^{-4} (or less) for all the governing equations.

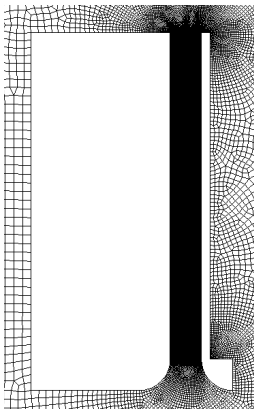

Figure 2 Meshing of the fluid domain

Validation of Numerical Models

Before beginning any studies on the dynamic behaviour of the flows, it is necessary to check that the numerical model developed is reliable. To perform this step, numerical results are compared with experimental data (Ospir et al. [10]). The dynamic flow structure was characterized experimentally by laser tomography utilizing discrete tracers, which are fine Rilsan® spherical particles, whose density is close to that of water (ρ=1060 kg/m^3). This visualization technique allows giving the streamline patterns deduced from the flow velocity field materialized by the trajectories of tracers during a long exposure time of the camera.

In the figure 3(a) a comparison of the streamlines between experimentation and numerical simulation is made for the same geometrical and thermal configuration (case 1) at a modified Rayleigh number of $4.5.10^6$ (ϕ=510 W/m^2) at t=30min which seems to be a sufficient time to reach the establishment of a steady-state flow.

In this comparison study, one may observe that the dynamical flow structures are similar, namely composed by a boundary layer upward flow near the heated wall and a recirculation zone at the channel outlet.

Even if the present study aims at considering a sole channel aspect ratio (R_f = 5.2), a complementary quantitative comparison between experimental and numerical experiments on the recirculation lengths was conducted for Ra* = $4.5.10^6$ and different R_f (Fig. 3(b)). One can observe that both numerical and

experimental recirculation sizes are very close with a maximum uncertainty of 6%.

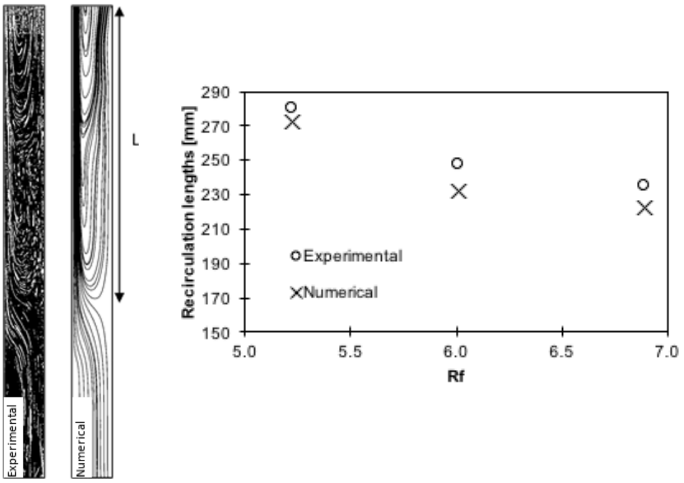

(a) (b)

Figure 3 Model validation for Ra*=4.5.10^6: (a) Flow structure ; (b) Recirculation lengths

RESULTS AND DISCUSSION

The flow dynamics and heat transfer in the asymmetrically heated vertical channel are investigated numerically. The study focuses specifically on the influence heat source distribution at heated wall. Only the convective aspects related to natural convection are studied by carrying out numerical simulation in a tank filled with water, which allows neglecting the radiation. 2D numerical results were obtained in the form of streamline patterns of the natural convection flow dynamics in the mid-plane of the asymmetrically vertical channel, over its entire height (2A) after 30 minutes of heating [10] which is a sufficient time to reach the establishment of a steady-state flow for such a configuration for Ra* = 4.5.10^6.

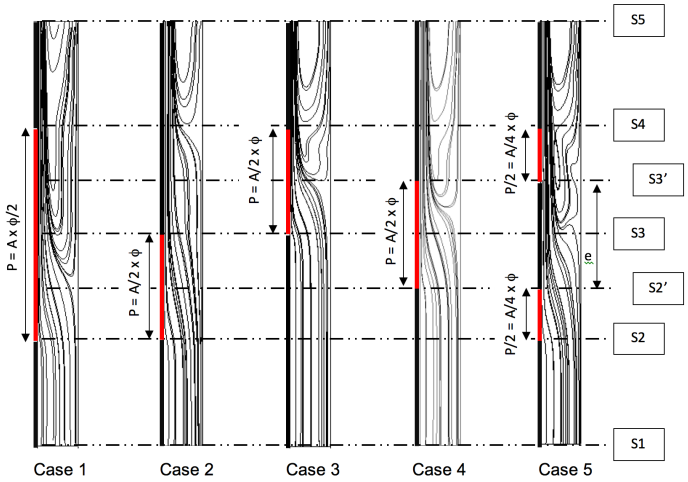

Figure 4 Streamline patterns in steady state

In Figure 4, one may observe a boundary layer-type flow which develops near the heated wall due to the fluid alimentation from the bottom of the channel. In the same time, cooler ambient fluid enters the channel from the upper side of the adiabatic wall. This leads to the formation of a recirculation zone, which can be observed at the channel outlet, near the adiabatic wall. In some cases, the thermosyphon loop gives rise to a vortex structure characterized by two large recirculation cells, connected by a neck and forming an elongated eight-shaped structure (cases 5). This thermosyphon loop extends over a distance of up to more than half of the channel height (case 1). It is noticed that the eight-shaped structure observed in case 5 has already been highlighted experimentally [10]. To analyse the flow in the channel, different observation sections (S1, S2, S3, S4, S5) have been introduced (fig. 4). Sections S1, S3 and S5 correspond respectively to the inlet, middle and outlet of the channel. Sections S2 and S4 correspond to heights of A/2 and 3A/2 respectively.Figure 5 presents the axial velocity (Vy) profiles at the channel entry (section S1) for the five cases. One may observe a parabolic profile for the axial velocity whatever the heating distribution is. In cases 2, 4 and 3, one may note that the more the beginning of the heated zone is close to the channel inlet, the more velocities are high [15-16]. Figure 5 shows also that when the heating source is divided (passage of case 4 in case 5) for a same flux density and with a same power, the velocities increase in accordance with [14].

At this section one may observe parabolic laminar Poiseuille-type profiles, which tend to flatten in the channel center when the heat source is located toward the channel bottom (cases 2 and 5). Nevertheless, it appears significant disparities in the value of the maximum velocity. Moreover, one can see that the more the incident flux density is high and concentrated in the lower part of the channel, higher the maximum velocity is.

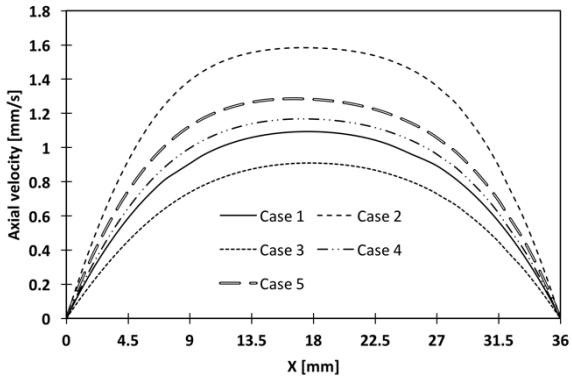

Figure 5 Vertical velocity in section S1 for Ra* = 4.5.10^6

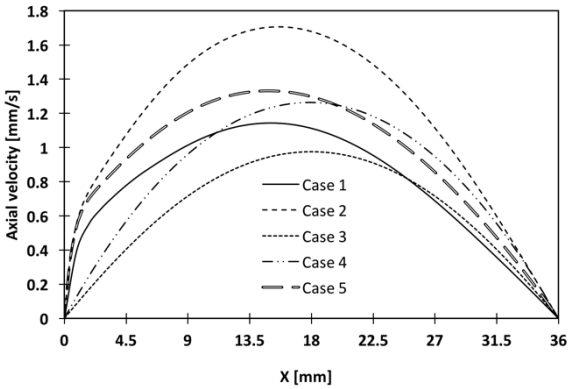

Figure 6 Vertical velocity in section S2 for Ra* = 4.5.10^6

Figure 6 shows the velocity profiles in Section 2. In this figure one can see parabolic velocity profiles for cases 3 and 4. However, for cases 1, 2 and 5 where the heating process occurs at this location, the maximum velocity is shifted to the hot wall of the channel. Consequently, the observed change in the slope at the origin is certainly due to the initiation of the thermal boundary layer having the effect of accelerating the flow in the vicinity of the heated wall. One may also note in section 2, an identical distribution of the velocity profiles as in section 1, namely greater velocities for case 2 and lower velocities for case 3. For the cases were the heating zone starts in section S2 (cases 1, 2 and 5) the inlet parabolic velocity profiles are modified due to the development of a thermal boundary layer.

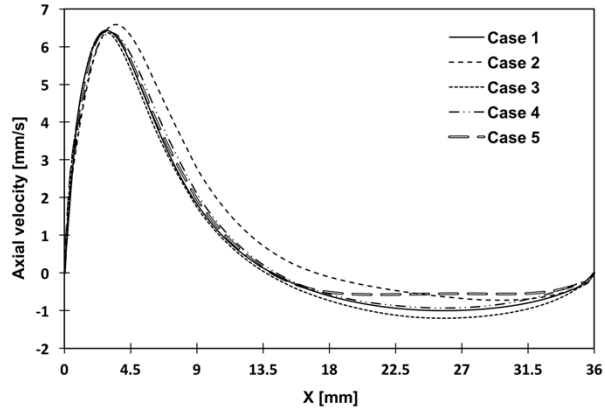

Figure 7 Vertical velocity in section S5 for Ra* = $4.5.10^6$

One may find that in Figure 7 corresponding to study area approaching the exit of the channel, the convection flow acts like a fully developed boundary layer one whatever the case studied. The position and layout of heat sources then tend to not have any influence on the profiles of the vertical velocities near the heated wall. In addition, the same width of the recirculation zone is observed for cases 1, 3, 4 and 5.

In conclusion, one may observe that this upper adiabatic zone tends to erase differences on the maximum velocities values while on the contrary the presence of an adiabatic zone at the channel inlet tends to accentuate them (zones S1 and S2).

In table 1, the mass flow rate has been calculated at the channel inlet for Ra*=$4.5.10^6$. One may note that case 3 is the case where the mass flow rate is the lowest. It corresponds to the case where the heating is focused at the upper half part of the channel while case 2, where the heating is focused on the downer half part of the channel, gives a higher mass flow rate. This confirms the observed trends in the velocity profiles obtained in sections S1, S2 and S4. Moreover, if cases 1, 4 and 5 are compared, one may note that the spacing between the heating sources influences the mass flow rate through the channel. For equal thermal power incident with a heating zone located in the middle of the channel (cases 1 et 4), decreasing the length of the heated zone leads to increase the mass flow rate up to 7%. Comparing cases 2, 3 and 4 which present an equivalent heating length it is found that the more the heating area is located close to the channel inlet, higher the mass flow rate is, in accordance with results obtained by Menezo et al. [16]. For example, there is an increase of the mass flow rate between cases 2 and 3 in the order of 46%. Relating cases 4 and 5 which have a symmetrical heating of the same length, it is found that spreading heat sources (e = 0 for case 4 and e = A/2 for case of 5) allows to increase the mass flow rate up to 10%. Similar trend has already been mentioned by Dehghan et al. [14]. According to Table 1, there is a strong relationship between the recirculation length and the average Nusselt number. It is observed that the heat transfer is maximal for the case 1 which has the longest recirculation zone.

Numerical cases	L, separation length (m)	$\overline{Nu}$	Mass flow rate [g/s]
1 (Ref)	0.229	20.0	28.2
2	0.093	12.1	42.4
3	0.143	12.9	23.0
4	0.165	12.9	30.5
5	0.179	14	33.9

Table 1 Thermal and dynamic behaviour for Ra* = $4.5.10^6$

Figure 8 represents the evolution of the wall temperature along the left heated wall. One may note that for all studied cases the evolution of the parietal temperature along the heat sources acts like a "1/4" power law as found for uniform heat flux (UHF) in natural convection flow on a vertical plate in an infinite medium, followed by a thermal relaxation zone.

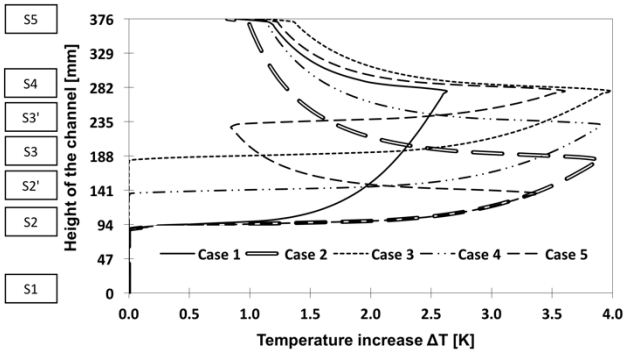

Figure 8 Temperature profiles at the channel heating wall for Ra* = $4.5.10^6$

One notices a very similar behaviour for cases 2, 3 and 4 having the same heating length. However, it is noted that the maximum temperature value increases when the heat source is close to the channel outlet. The observed difference in temperature is then about for 4%. When the length of the heated zone is doubled with a lower flux density as in case 1, there is a situation where the temperatures are lower. Moreover, for case 5 with a heat source-spreading situation one can observe a

sawtooth-shaped temperature profile having the effect of decreasing the maximum temperature on the heated wall.

CONCLUSION

This numerical study was focused on both heat transfer and flow dynamics resulting from varying heat source position at wall in an asymmetrically heated vertical channel. In order to neglect radiation, only the convective aspects related to natural convection are studied by carrying out simulations in water.

This study has highlighted that the heat distribution has a strong impact on the flow structure and convective heat transfer in an asymmetrically heated vertical channel. The conclusions are as follows:

- decreasing the length of the heated zone and simultaneously increase the heat flux density leads to increase the mass flow rate.
- the more the heating area is located close to the channel inlet, higher the mass flow rate is.
- spreading heat sources allows to increase the mass flow rate
- upper adiabatic zone tends to erase differences on the maximum velocities values while on the contrary the presence of an adiabatic zone at the channel inlet tends to accentuate them
- the more the position of the heating source is lower in the channel, the more mass flow rate coming in through the bottom of the channel is important.
- the heating source separation increases convective heat transfer
- a strong relationship between the recirculation length and the average Nusselt number. It is observed that the heat transfer is maximal for the case 1 which has the longest recirculation zone.
- the distribution of heating sources at the bottom of the channel (case 2) allows to increase the mass flow rate through the channel.

ACKNOWLEDGMENTS

This work is financially supported by the European Union (EU) through the European Regional Development Fund (FEDER), the Champagne-Ardenne region and the company CAMPA as part of Effi-SiEMCE project.

REFERENCES

[1] Ding W., Hasemi Y., Yamada T., Natural ventilation performance of a double-skin facade with a solar chimney, Energy and Buildings Vol. 37, 2005, pp. 411-418.

[2] Gan G., A parametric study of Trombe walls for passive cooling of buildings, Energy and Buildings, Vol. 27, 1998, pp. 37-43.

[3] Elenbaas W., Heat dissipation of parallel plates by free convection, Physica, Vol. 9, 1942, pp. 1-28.

[4] Webb B.W., Hill D.P., High Rayleigh number laminar natural convection in an asymmetrical heated vertical channel, ASME J. Heat Transfer, 1989, pp. 649-656.

[5] Wirtz V, Stutzman R.J., Experiments on free convection between vertical parallel plates with symmetric heating, ASME J. Heat Transfer, 1982, pp. 501-507.

[6] Sparrow E.M., Chrysler G.M., Azevedo L.F., Observed flow reversals and measured-predicted Nusselt numbers for natural convection in a one-sided heated vertical channel, ASME J. Heat Transfer, 1984, pp. 325-332.

[7] Yilmaz T., Gilchrist A., Temperature and velocity field characteristics of turbulent natural convection in a vertical parallel-plate channel with asymmetric heating, Heat Mass Transfer, 2007, pp. 707-719.

[8] Dupont F., Ternat F., Samot S., Blonbou R., Two-dimension experimental study of the reverse flow in a free convection channel with active walls differentially heated, Experimental Thermal and Fluid Science, Vol. 47, 2013, pp. 150-157.

[9] Manca O., Morrone B., Naso V., A numerical study of natural convection between symmetrically heated vertical parallel plates, Proceedings XII Congresso Nazionale sulla Trasmissione, 1994, pp. 379-390.

[10] Ospir D., Popa C., Chereches N.C., Polidori G., Fohanno S., Flow visualization of natural convection in a vertical channel with asymmetric heating, International Communications in Heat and Mass Transfer, 2012, pp. 486-493.

[11] Li R., Bousetta M., Chenier E., Lauriat G., Effect of surface radiation on natural convective flows and onset of flow reversal in asymmetrically heated vertical channels, International Journal of Thermal Sciences, 2013, pp. 9-27.

[12] Popa C., Ospir D., Fohanno S., Chereches N.C., Numerical simulation of dynamical aspects of natural convection flow in a double-skin façade, Energy and Buildings, 2012, pp. 229-233.

[13] Christian S., Patrice J., José L.M., Francisco S.J., Heat transfer and mass flow correlations for ventilated facades, Energy and Buildings Vol. 43, 2011, pp. 3696–3703.

[14] Dehghan A.A., Behnia M., Numerical investigation of natural convection in a vertical slot with two heat source elements, International Journal of Heat and Fluid Flow, Vol. 17, 1996, pp. 474-482.

[15] Fossa M., Ménézo C., Leonardi E., Experimental natural convection on vertical surfaces for building integrated photovoltaic (BIPV) applications, Experimental Thermal and Fluid Science, Vol. 32, 2008, pp. 980–990.

[16] Ménézo C., Fossa M., Leonardi E., An experimental investigation of free cooling by natural convection of vertical surfaces for building integrated photovoltaic (bipv) applications. In Thermal Issues in Emerging Technologies, ThETA 4, Cairo, Egypt Jan 3-6th, January 2007, number 1, p. 7.

[17] Desrayaud G., Chénier E., Joulin A., Bastide A., Brangeon B., Caltagirone J.P., Cherif Y., Eymard R., Garnier C., Giroux-Julien S., Harnane Y., Joubert P., Laaroussi N., Lassue S., Le Quéré P., Li R., Saury D., Sergent A., Xin S., Zoubir A., Benchmark solutions for natural convection flows in vertical channels submitted to different open boundary conditions, International Journal of Thermal Sciences Vol. 72, 2013, pp.18-33.

[18] Garnier C., Modélisation numérique des écoulements ouverts de convection naturelle au sein d'un canal vertical asymétriquement chauffé, PhD These (2014), University of Pierre et Marie Curie, France.

[19] Polidori G., Fatnassi S., Ben Maad R., Fohanno S., Beaumont F., Early-stage dynamics in the onset of free-convective reversal flow in an open-ended channel asymmetrically heated, International Journal of Thermal Sciences, Vol. 88, 2015, pp. 40-46.

[20] Gray D.D., Giorgini A., The validity of the Boussinesq approximation for liquids and gases, Int. J. Heat Mass Transfer, 1976, pp. 545-551.

[21] Bejan A., Convection Heat Transfer, Wiley-Interscience 1984.

[22] Patankar S.V., Numerical Heat Transfer and Fluid Flow, Hemisphere, Washington, DC, 1980.